Identification of the P2Y$_{12}$ receptor in nucleotide inhibition of exocytosis from bovine chromaffin cells

Steven J. Ennion*, Andrew D. Powell* and Elizabeth P. Seward

* These authors contributed equally to the work.

Department of Cell Physiology and Pharmacology, University of Leicester, (SJE),

Department of Pharmacology, University of Bristol, (ADP), Department of Biomedical

Sciences, University of Sheffield (EPS).

Running Title: P2Y$_{12}$ mediated inhibition of exocytosis

Corresponding author:

Dr Elizabeth P. Seward

Institute of Molecular Physiology,

University of Sheffield,

Alfred Denny Building,

Western Bank,

 Sheffield,

S10 2TN, U.K.

Tel: (44) 114-222-2383   FAX: (44) 114-222-2360

E-mail: e.p.seward@sheffield.ac.uk

Text pages: 31

Tables: 2

Figures: 8

References: 40

Words in Abstract (250 word limit): 197

Words in Introduction (750 word limit): 633

Words in Discussion: (1500 word limit): 1312

Non-standard abbreviations:

VOCC: Voltage operated Ca^{2+} channel
I$_{Ca}$: Ca^{2+} current
C$_m$: membrane capacitance
PPADS: Pyridoxal-phosphate-6-azophenyl-2',4' disulfonic acid
2-MeSATP: 2-methylthioadenosine 5'- triphosphate
2-MeSADP: 2-methylthioadenosine 5'- diphosphate
PTX: Pertussis toxin
ARC69931MX: N^6-(2-methylthioethyl)-2-(3,3,3-trifluoropropylthio)-β,γ-dichloromethylene ATP

ABSTRACT

Nucleotides are released from bovine chromaffin cells and take part in a feedback loop to inhibit further exocytosis. In order to identify the nucleotide receptors involved, we measured the effects of a range of exogenous nucleotides and related antagonists on voltage-operated calcium currents (I_{Ca}), intracellular calcium concentration ($[Ca^{2+}]_i$), and membrane capacitance changes (ΔC_m). In comparative parallel studies we also cloned the bovine $P2Y_{12}$ receptor from chromaffin cells, and determined its properties by co-expression in *Xenopus* oocytes with inward- rectifier potassium channels made up of Kir3.1 and Kir3.4. In both systems, the agonist order of potency was essentially identical (2-MeSATP≈2-MeSADP>>ATP≈ADP>UDP). αβMethylene-ATP and adenosine were inactive. UTP inhibited I_{Ca} in chromaffin cells (pEC_{50} 4.89 ± 0.11) but was essentially inactive at the cloned $P2Y_{12}$ receptor. The relatively non-selective P2 antagonist pyridoxal-phosphate-6-azophenyl-2',4' disulfonic acid (PPADS) blocked nucleotide responses in both chromaffin cells and Xenopus oocytes, whilst the $P2Y_{12}$ and $P2Y_{13}$ selective antagonist, ARC69931MX blocked responses to ATP in both chromaffin cells and Xenopus oocytes but not to UTP in chromaffin cells. These results identify the $P2Y_{12}$ purine receptor as a key component of the nucleotide inhibitory pathway, and also demonstrate the involvement of a UTP sensitive $G_{i/o}$ coupled pyrimidine receptor.

Given the profusion of P2 nucleotide receptors in the nervous system and the many pathways for nucleotide release, the potential for extracellular nucleotides to play a major modulatory role in neurotransmission is high. Based on their structure and signalling mechanisms, P2 receptors are classified as either ligand gated $P2X_{1-7}$ cation channels or as metabotropic $P2Y_{1,2,4,6,11-15}$ receptors coupled to heterotrimeric G proteins (North, 2002; Abbracchio *et al.*, 2003, Inbe *et al.*, 2004). Activation of P2X receptors by ATP leads directly to membrane depolarisation and calcium entry both via the P2X channels themselves and also by the subsequent activation of VOCCs (voltage-operated calcium channels) (North, 2002). P2Y receptors have a wider agonist profile than the P2X receptors responding to purines, pyrimidines and UDP-glucose. These receptors can be divided into two subgroups based on their molecular structure and coupling to Gα-subunits, with $P2Y_{12}$, $P2Y_{13}$ and $P2Y_{14}$ making up one group which signal via PTX-sensitive $G_{i/o}$ proteins , and $P2Y_1$, $P2Y_2$, $P2Y_4$, $P2Y_6$, $P2Y_{11}$ and $P2Y_{15}$ making up the second group, coupling to phospholipase C and G proteins of the G_q- class (Abbracchio *et al.*, 2003; Inbe *et al.*, 2004).

In the sympathetic nervous system, the effects of presynaptic purine receptors on neurotransmission have been well documented; facilitation of catecholamine release is mediated by P2X receptors, whilst inhibition is mediated by the activation of an unidentified P2Y receptor (Von Kügelgen *et al.* 1989; Boehm and Kubista, 2002). Evidence for inhibitory presynaptic P2Y receptor(s) regulating release of catecholamine as well as other neurotransmitters in the central nervous system is also accumulating (Cunha and Ribeiro 2000; Zhang *et al.* 2003). Identifying which nucleotide receptor subtypes mediate presynaptic inhibition has been complicated by the inaccessibility of the majority of mammalian nerve terminals, complexity arising from neural circuits where multiple P2 receptors may be activated, stimulation of P1 adenosine receptors following breakdown of purines by

4

ectonucleotidases, and the limited availability of P2 receptor subtype selective agonists and antagonists.

Adrenal chromaffin cells are embryonically derived from precursors of sympathetic neurones, they also release catecholamines and ATP by Ca^{2+} regulated exocytosis and express inhibitory P2 receptors that couple to neuronal VOCCs (Diverse-Pierluissi *et al.* 1991; Gandia *et al.* 1993; Currie and Fox 1996). Moreover, evidence for an autocrine feedback loop similar to that proposed for sympathetic neurones involving an inhibitory P2Y-like receptor has been reported (Carabelli *et al.* 1998). In a previous study, we used combined C_m measurements and voltage-clamp recordings to examine the mechanisms underlying purinergic inhibition of exocytosis in chromaffin cells (Powell *et al.*, 2000). We showed that the purine analogue 2-MeSATP inhibits Ca^{2+} entry through N- and P/Q-type VOCCs and consequently, stimulus-evoked changes in C_m through a PTX-sensitive G protein. The aim of this study was to expand on this finding by determining the molecular identity of the P2Y receptor(s) involved. Here we provide evidence for two inhibitory PTX-sensitive $G_{i/o}$-coupled P2Y receptors in bovine chromaffin cells. One of these receptors shows a pharmacology similar, but not identical (ATP being a full agonist and equipotent to ADP) to the human $P2Y_{12}$ receptor, whilst the second receptor is UTP sensitive and hence shows a pharmacology not matching any of the known $G_{i/o}$-coupled P2Y receptors. In order to confirm the role of $P2Y_{12}$ in VOCC inhibition, we cloned the bovine $P2Y_{12}$ receptor from bovine chromaffin cells and expressed this receptor in *Xenopus* oocytes co-expressing inward- rectifier potassium channels made up of rat Kir3.1 and Kir3.4. The pharmacological properties of this cloned receptor closely mirrored the pharmacology observed in chromaffin cells except that UTP was a very weak partial agonist. We therefore conclude that $P2Y_{12}$ and another as of yet unidentified $G_{i/o}$-protein coupled UTP-sensitive receptor inhibit VOCCs and exocytosis in chromaffin cells.

These findings support the view that $G_{i/o}$ coupled P2Y receptors may also act as presynaptic inhibitory receptors in other neuronal systems to regulate neurotransmitter release.

MATERIALS AND METHODS

Chromaffin cell culture- Chromaffin cells were prepared by collagenase digestion of bovine adrenal glands as previously described (Powell *et al.*, 2000). Adrenal glands from 18-24 month old cows were obtained from a local abattoir and retrogradely perfused at 25 ml/min for 30 min at 37 ^{o}C with the digestive enzymes collagenase type 2 (0.03 %) (Worthington Biochemical Corp., Lakewood, NJ) and DNAse I (0.0013 %) (Boehringer Mannheim Biochemicals, Indianapolis) added to Locke's solution (154.2 mM NaCl, 2.6 mM KCl, 2.2 mM K_2HPO_4, 0.85 mM KH_2PO_4, 10 mM glucose, 5 mM HEPES, 0.0005 % Phenol Red (Gibco BRL, Paisley, UK); pH adjusted to 7.2 with NaOH). After surgical removal of the cortex, the medulla was dissected, cut into small pieces, placed in a trypsinisation flask with fresh enzyme solution and stirred at slow speed for 30 min at 37 ^{o}C. Cells were washed twice with Earle's Balanced Salt Solution (Gibco BRL) and resuspended in Dulbecco's Modified Eagle's Medium (DMEM; Gibco BRL) supplemented with 44 mM $NaHCO_3$, 15 mM HEPES, 10% fetal calf serum (Gibco BRL), 1% glutamine, 1% penicillin-streptomycin solution, 2.5 mg/ml gentamycin, 0.5 mg/ml 5`-fluorodeoxyuridine, and 0.01 mg/ml cytosine-β-δ-arabino-furanoside. Cells were plated on glass cover slips coated with matrigel (Becton Dickinson Labware, Bedford, MA) at an approximate density of 800 cells/mm^2. Approximately 80% of the media was replaced 24 hr after plating and cells were maintained for up to 7 days in a humidified atmosphere of 95% O_2 / 5% CO_2 at 37 ^{o}C.

$[Ca^{2+}]_i$ measurements in bovine chromaffin cells- Cells were loaded with the Ca^{2+} indicator Fura 2-AM by addition of 5 μM Fura-2/AM (Molecular Probes) to DMEM medium and

incubated for 25 min at 37 ℃. Cells were then washed with fresh DMEM and incubated a

further 15 min at 37 ℃. Isolated fluorescent chromaffin cells were alternately illuminated at

340 nm and 380 nm using a monochromator (TILL Photonics, Gräfelfing, Germany)

controlled by the data acquisition software. Emission >430 nm was collected with a

photomultiplier tube (TILL Photonics) and sampled approximately every 12 ms. Data were

stored on PC and ratios of 340/380 nm were calculated off-line (Axobasic-written software).

Electrophysiological recordings in bovine chromaffin cells- A cover slip carrying chromaffin

cells was placed in a micro-perfusion chamber (~200µl volume) on the stage of an inverted

phase-contrast microscope (Nikon, Diaphot 200). Cells were continuously superfused with an

external solution consisting of 130 mM NaCl, 2 mM KCl, 1 mM $MgCl_2$, 5 mM $CaCl_2$, 10 mM

glucose and 10 mM HEPES, adjusted to pH 7.2 with NaOH, osmolarity ~280 mOsm. Special

care was taken to superfuse cells at a high rate (~ 3 ml/min) throughout the experiment and to

select well isolated single cells for recording in order to avoid compounding effects of

endogenously released modulators (Carabelli *et al.*, 1998). Ionic currents were recorded in

whole-cell or perforated patch clamp configuration using borosilicate glass electrodes coated

with Sylgard 184 (Dow Corning, Midland, MI) and fire polished on a microforge to a

resistance of 1-2 MΩ. Electrodes were filled with an internal solution consisting of 145 mM

Cs-glutamate (Calbiochem, Nottingham, UK), 10 mM HEPES, 9.5 mM NaCl, 0.3 mM bis(2-

aminophenoxy)ethane-N,N,N',N'-tetra-acetic acid (BAPTA; Molecular Probes, Eugene, OR),

adjusted to pH 7.2 with CsOH (ICN Biomedicals Inc., Aurora, OH); osmolarity ~ 280 mOsm.

For whole-cell recording experiments, 2mM Mg-ATP was added to the internal solution to

prevent rundown of VOCCs and exocytosis. Gramicidin D (Sigma, Poole, U.K.) at a final

concentration of 9.7 µg/ml was used for perforation. For both whole-cell and perforated-patch

recordings, series resistance was less than 12 MΩ and compensated (typically > 70%)

electronically with the patch-clamp amplifier (Axopatch 200B; Axon Instruments, Foster City, CA). Voltage protocol generation and data acquisition were performed using custom data acquisition software (kindly provided by Dr. A. P. Fox, University of Chicago) running on a Pentium computer equipped with a Digidata 1200 acquisition board (Axon Instruments). Current traces were low pass filtered at 5 kHz using the four-pole Bessel filter of the amplifier and digitized at 10 kHz. Chromaffin cells were voltage-clamped at -90 mV and C_m was sampled with a resolution of 12 ms using a software-based phase-tracking method as described previously (Fidler and Fernandez, 1989; Powell *et al.*, 2000). Data were stored on the computer hard drive and analysed off-line using self-written (Axobasic; Axon Instruments) and commercial (Origin, Microcal, Northampton, MA) software. All experiments were performed at ambient temperature (21-25°C).

Cloning of the bovine P2Y$_{12}$ receptor- The strategy used to clone the bovine P2Y$_{12}$ receptor consisted of three sequential rounds of cloning. Firstly a conserved central region of the receptor was amplified by PCR (Polymerase chain reaction) with degenerate primers (PCR1). Secondly, 5' and 3'RACE (Rapid amplification of cDNA ends) primers were designed from the sequence obtained from PCR product 1 and used to amplify the 5' and 3' ends of the receptor by 5' and 3' RACE respectively (PCRs 2 and 3). Finally, sequence obtained from PCR products 2 and 3 was used to design primers to amplify the full length receptor from bovine chromaffin cell cDNA by RT-PCR. A proof reading polymerase (Bio-X-Act, Bioline, U.K) was used for all PCR reactions. Total RNA was prepared from bovine chromaffin cells and 5µg was used in a first strand cDNA reaction using RoRidT$_{(17)}$ primer (Harvey and Darlison, 1991) and Superscript II reverse transcriptase according to the manufacturers instructions (Amersham, U.K.). The degenerate primers for PCR 1, y12degF (5'TTTCTGTTGYCATCTGGCCMTTCATG 3') and y12degR

(5'GGTCACCACCWTCYTGTYCTTTYTTC 3') were designed based on homologous regions of the human mouse and rat $P2Y_{12}$ sequences (Accession numbers NM_022788, AK013804 and NM_022800 respectively). 5' RACE (PCR 2) was performed using a SMART^{TM} RACE kit (Clontech U.S.A) according to the manufacturers instructions with the sequence specific primer TEW81 (5' GCCAAACCAGACCAAACTCTGACTTCAG 3') designed from the sequence of PCR 1. 3' RACE (PCR 3) was performed utilising the primers Ro (Harvey and Darlison, 1991), and bY12RACEfor (5' GGTGCTGGCAAAGTCCCCAAGAA 3'). The primers 2ndby12fullfor (5' GACGGAAATACAGTGTCTGC 3') and 2ndby12fullrev (5' CTTGCCTTTGGGGAGTT 3') were designed from the sequence obtained from PCRs 1 and 2 and utilised in RT-PCR to amplify the full length $P2Y_{12}$ receptor from first strand cDNA prepared from bovine chromaffin cells. PCR products were cloned into the plasmid pCDNA3 (Invitrogen USA) and two independent colonies sequenced on both strands (Automated ABI sequencing service, Protein and Nucleic acid Laboratory, University of Leicester).

RT-PCR analysis- RT-PCR was performed on first strand cDNA prepared from bovine chromaffin cells as described above. The only published bovine P2Y sequence available for primer design was that of $P2Y_1$ (Henderson *et al.*, 1995). BLAST homology searches of the bovine EST database found sequences corresponding to the bovine $P2Y_{2, 6 \text{ and } 14}$ receptors (Accession numbers BM031311, BI680595 and CB429080 respectively). Allowing the presence of transcripts for $P2Y_{1, 2, 6, 12, \text{ and } 14}$ to be analysed in addition to the published bovine $P2Y_1$ (Primer sequences in Table 1).

Electrophysiological recordings in Xenopus oocytes- Xenopus oocytes expressing the rat inwardly rectifying potassium channels Kir 3.1 and Kir 3.4 were used to assess the function of

the cloned bovine $P2Y_{12}$ receptor in a system similar to that utilised by Hollopeter and co-workers to characterise the human $P2Y_{12}$ receptor (Hollopeter *et al.*, 2001). Plasmids for rat Kir 3.1 and Kir 3.4 were a kind gift from Prof M. Boyett. cRNA was transcribed from linearized $P2Y_{12}$, Kir 3.1 and Kir 3.4 plasmids using the mMessage mMachine^{TM} system (Ambion, U.S.A) according to the manufacturers instructions. De-folliculated stage V-VI *Xenopus* oocytes were injected with 1.25ng Kir 3.1, 1.25ng Kir 3.4 and 50 pg $P2Y_{12}$ cRNA in a total volume of 50 nl using an Inject +Matic micro injector (J.Alejandro Gaby, Genéva). Oocytes were stored at 18 ^{o}C in ND96 buffer (96 mM NaCl, 2 mM KCl, 1.8 mM $CaCl_2$, 1 mM $MgCl_2$, 5 mM sodium pyruvate, 5 mM HEPES, pH 7.6) prior to use 3-7 days later.

Two-electrode voltage clamp recordings were made from oocytes using a Turbo TEC 10C amplifier (NPI Electronic Instruments, Germany) with a Digidata 1200 analogue to digital converter (Axon Instruments U.S.A.) and WinWCP acquisition software (Dr J. Dempster University of Strathclyde, Scotland). Agonists and antagonists were bath perfused using a custom built rapid exchange perfusion system. Oocytes were initially perfused with ND96 in order to obtain a value for the resting membrane potential (typically ~ -70mV for Kir injected oocytes, and ~ -20mV for non-injected or $P2Y_{12}$ only injected oocytes) before exchange to 70K solution (20mM NaCl, 70mM KCl, 3 mM $MgCl_2$ 5mM HEPES) for recording of agonist evoked membrane currents. Agonist evoked currents could be measured in oocytes clamped constantly at – 60mV, however, the current required (~5 µA) to clamp at this potential tended to kill cells after ~15-30 minutes. Therefore, in order to obtain full concentration response curve data for individual cells, oocytes were clamped at 0 mV during the initial period of agonist application and in recovery periods between applications. One minute after agonist application commenced, the holding potential was stepped down to -60mV for 5 seconds and the peak current recorded. A ramp from -60mV to +90mV over 2 seconds was applied after the 5 second recording period in order to visualise the inward

rectification from the Kir channels, verifying that the cell was still in a healthy condition. Currents in the presence of agonist were normalised to the mean of recordings taken 5 minutes prior and 5 minutes after in the absence of agonist.

All drugs were made up as concentrated stock solutions in distilled water and stored in aliquots at –20 ℃ until use. Stocks were thawed once and diluted into the superfusing solution. Nucleotide analogues were obtained from Sigma (Poole, U.K.). 2-Methylthio ATP (2-MeSATP) and Pyridoxalphosphate-6-azophenyl-2',4'-disulphonic acid (PPADS) were obtained from Tocris Cookson (Bristol, U.K). PTX (Sigma) was dissolved in 50% Glycerol containing Tris 50mM, Glycine 10mM, NaCl 0.5M, pH 7.5.

Data analysis- Ca^{2+} entry in chromaffin cells was determined by integration of I_{Ca}, the left limit was set ~ 3 ms into the voltage pulse, to exclude the major portion of the contaminating Na^+ current. ΔC_m measurements were performed as described previously (Powell *et al.* 2000). Concentration response data obtained from individual cells were fitted with the Hill equation: $Y = ((X)^H.M)/((X)^H + (EC_{50})^H)$ where Y = response, X = agonist concentration, H is the Hill coefficient, M is maximum response and EC_{50} is the concentration of agonist evoking 50% of the maximum response. pEC_{50} is the $-\log_{10}$ of the EC_{50} value. Data are presented as mean $\pm$ s.e.m. and differences between means were tested using either paired or independent Student's t-test, as appropriate.

RESULTS

Measurements of I_{ca} in chromaffin cells. The effects of adenosine and uridine nucleotides on I_{Ca} in bovine chromaffin cells were examined (Figure 1). Currents were activated every 30 sec with step depolarizations to +20 mV from a holding potential of -90 mV. Superfusion with ATP or the P2Y selective analogue, 2-MeSATP had no effect on the holding current but reversibly inhibited I_{Ca} by 45 ± 3 % (100 μM ATP, n=13) and 44 ± 4 % (100 nM 2-MeSATP, n=11). UTP (100μM) also inhibited I_{Ca} (36 ± 6 %, n=11) without changing the holding current. Preceding the test pulse by a 20 ms depolarizing prepulse to 120 mV reduced the inhibitory effect of 2-MeSATP to 15.5 ± 3.5 % (n=3) and of UTP to 8 ± 2% (n=3) (Figure 1C). The voltage-dependence of the inhibitory effect was also observed by examining the effect of 2-MeSATP on the current-voltage relationship (data not shown). Inhibition of I_{Ca} by 2-MeSATP was significantly reduced at potentials positive to +30 mV. Furthermore, 2-MeSATP produced a significant depolarizing shift in the activation curve (V_{50} control 14.8 ± 3.7 mV, 2-MeSATP 22.4 ± 4.7 mV, n=6 p<0.05). The voltage-sensitivity of the inhibitory effects of the purines and pyrimidines on I_{Ca} is consistent with a signalling pathway that involves direct modulation of the channels by $G_{\beta\gamma}$ subunits (Dolphin, 2003). Treatment of chromaffin cells with PTX (250 ng/ml for 24 hours) completely blocked the effect of both 2-MeSATP (3.5 ± 0.8%; n=4) and UTP (2.8 ± 1.0 %, n=4) (Figure 1D,E), confirming the sole involvement of $G_{i/o}$ coupled P2Y receptor(s) in the modulation of I_{Ca}. In contrast to heterologously expressed $P2Y_4$ receptors (Filippov *et al.*, 2003), the inhibition produced by UTP in chromaffin cells was not sensitive to cell dialysis; application of 30μM UTP (~EC_{50} concentration) inhibited I_{Ca} recorded in the whole-cell configuration by 15.2 ± 2.1 % (n=6) and by 16.3 ± 3.1 % (n= 8) in the perforated-patch configuration.

12

Involvement of Ca^{2+} mobilising P2Y or P2X receptors in VOCC inhibition. To investigate the possible contribution from Ca^{2+} mobilizing P2 receptors to inhibition of VOCCs, we loaded chromaffin cells with the Ca^{2+}-sensitive dye Fura-2 to monitor [Ca^{2+}]$_i$. In 10 out of 12 cells examined, neither ATP (100μM) nor UTP (100μM) produced any increase in [Ca^{2+}]$_i$; in these same cells, histamine (100μM) and Angiotensin II (300nM), agonists known to activate PLC coupled receptors in chromaffin cells (Cheek *et al.*, 1993;Teschemacher and Seward, 2000), produced robust increases in [Ca^{2+}]$_i$ (Figure 2). Superfusion with 2-MeSATP (100 nM) also failed to produce any significant change in basal [Ca^{2+}]$_i$ (n = 4; see also Figure 1 Powell *et al.* 2000). In two out of 12 cells, ATP produced a small increase in [Ca^{2+}]$_i$ (mean 186% of control). However, both of these cells were found to be relatively unresponsive to histamine (mean value of 124% of control compared with 279% for ATP/UTP non-responsive cells) and had approximately half the diameter of chromaffin cells usually selected for electrophysiological investigation. (mean membrane capacitance 7.7 ± 0.5 pF (n=20), corresponding to diameter of ~15 μm). Whether this minor population of cells corresponds to noradrenergic or cortical cells, which make up 10-20% of adrenal medullary cultures, was not investigated further. From these results we can conclude that neither Ca^{2+} mobilizing P2X receptors nor PLC-coupled P2Y$_{1,2,4,6}$ receptors are functionally detectable in the majority of chromaffin cells.

Agonist profile of P2Y receptors in chromaffin cells. The relative paucity of high affinity subtype selective ligands complicates the unambiguous identification of P2Y receptors within intact tissues. The method most commonly utilised to identify native P2Y receptors is to examine the relative order of potency of numerous purine and pyrimidine analogues. We examined the efficacy of a number of commonly used purine and pyrimidine analogues to inhibit I$_{Ca}$ in chromaffin cells. Agonist profiling yielded an agonist order of potency of 2-

MeSATP $\approx$ 2MeSADP >> ATP $\approx$ ADP $\geq$ ATPγS > UTP $\geq$ UDP (Figure 3A). $\alpha\beta$Methylene-ATP and adenosine were inactive (100 μM, data not shown). 2-MeSATP, 2-MeSADP, ATP, ADP and ATPγS were full agonists with mean EC$_{50}$ values of (in nM): 0.49 (n=4) ,0.73 (n=4), 347 (n=4), 387 (n=3) and 1170 (n=3) and Hill slopes of approximately 1 (Table 2).

The uridine nucleotides were less potent than the adenosine analogues (Table 2) and UTP was incapable of exerting a full inhibitory response (Figure 3A), suggesting that it may act as a partial agonist on a receptor with mixed purine/pyrimidine sensitivity. To test this possibility, the effects of co-application of a sub-maximal concentration of UTP (10 μM) with 2-MeSATP (10 pM - 10 nM) were tested. If UTP were acting as a partial agonist at the same receptor population as those activated by 2-MeSATP, co-application would be expected to cause a rightwards shift in the concentration response curve and a depression of the maximal response. The IC$_{50}$ for 2-MeSATP alone and in the presence of UTP (10 μM) however, were similar (0.22 and 0.16 nM, Figure 3B), and although a slight decrease in the maximal response was observed (2-MeSATP alone, 48 $\pm$ 3 % and 2-MeSATP and UTP, 45 $\pm$ 6 %, n=4), this was not significant ($p = 0.66$).

In response to prolonged activation many G-protein coupled receptors undergo desensitisation; UTP preferring P2Y$_4$ receptors can be distinguished from UDP preferring P2Y$_6$ receptors in that they show rapid desensitization (Brinson and Harden, 2001). Thus, to further characterize the UTP receptor in chromaffin cells, we examined the rate and cross-desensitization of nucleotide inhibition of I$_{Ca}$ (Figure 4). The general protocol to study desensitisation was an initial 3 minute application of either 2-MeSATP or UTP, to evaluate the control inhibition. Subsequent to this either 2-MeSATP or UTP was applied for 15 minutes and then washed out briefly, before 2-MeSATP and UTP were re-applied to check for cross-desensitisation. With prolonged superfusion of UTP, the inhibition of I$_{Ca}$ was reduced from 35 $\pm$ 9%, to 11 $\pm$ 6 % (Figure 4A). In the same cells, application of 2-MeSATP

14

inhibited I_{Ca} by 48 ± 6% and 49 ± 6% (n=4) before and after perfusion with UTP, showing

that the decline in I_{Ca} inhibition seen during perfusion with UTP was not due to rundown of

the channels but desensitisation of the receptor. Moreover, since the response to 2-MeSATP

was unaffected by desensitisation of the UTP response, we can conclude that there is no

cross-desensitisation of the purine and pyrimidine preferring receptors in these cells. The

desensitised response of UTP did not recover following an 11 minute wash period. In the

converse experiment it was noted that the inhibitory effect of 2-MeSATP on I_{Ca} did not

undergo such pronounced desensitisation (Figure 4B). 2-MeSATP maximally inhibited I_{Ca} by

43 ± 3%, during the 15 minute superfusion the mean inhibition was reduced to 29 ± 4%

(n=4). The response to a second application of 2-MeSATP after an 11 minute wash period

was back to 37 ± 6%. The size of the response to UTP (100 μM) was slightly decreased on the

second application (28 ± 13% versus 19 ± 9%, n=4) however, this was not significant.

Antagonist-sensitivity of P2Y receptors in chromaffin cells.   The agonist selectivity and

PTX-sensitivity of the P2Y receptor(s) expressed in bovine adrenal chromaffin cells do not

match that reported for any single cloned mammalian P2Y receptor. We therefore proceeded

to examine the antagonist selectivity of the receptor(s). PPADS has been shown to be an

antagonist at $P2Y_1$, $P2Y_2$, $P2Y_6$ and $P2Y_{13}$ receptors (Marteau *et al.*, 2003), but not at $P2Y_4$

receptors (Charlton *et al.*, 1996;Boyer *et al.*, 1994) or human $P2Y_{12}$ receptors (Takasaki *et al.*,

2001). PPADS antagonized the inhibitory effects of 2-MeSATP (1 nM) and UTP (30 μM) in

a reversible manner. Schild analysis of PPADS antagonism of 2-MeSATP inhibition of I_{Ca},

showed that the antagonist was acting in a competitive manner with an apparent pA_2 value of

6.42 ± 0.33 (Figure 5A). Examination of whether PPADS produced competitive antagonism

of the UTP-induced inhibition of I_{Ca} was not carried out because of the low potency of UTP.

Finally we examined the ability of the antithrombotic drug ARC69931MX, reported to be

15

selective for $P2Y_{12}$ and $P2Y_{13}$ receptors (Ingall *et al.*, 1999; Marteau *et al.*, 2003), to antagonize the regulation of I_{Ca} in chromaffin cells. Superfusion with ARC69931MX (1μM) for 1-3 minutes had no effect on I_{Ca} (106 ± 12 % of control, n=4), but in the same cells largely abolished the inhibition produced by ATP (100μM) from 49 ± 4% to 6 ± 5 % (n=4). Schild analysis of ARC69931MX antagonism of 2-MeSADP inhibition of I_{Ca} gave an apparent pA_2 value of 9.90 ± 0.06. Inhibition of I_{Ca} by 30μM UTP however persisted in the presence of ARC69931MX (mean 20 ± 9 %, n=3), supporting the notion that distinct ATP and UTP receptors are expressed by chromaffin cells.

Measurements of exocytosis in chromaffin cells. An increase in C_m follows vesicle fusion after Ca^{2+} entry and provides a measurement of exocytosis corresponding to 2fF per vesicle fusion. We therefore utilised C_m measurements to determine the effects of VOCC inhibition by nucleotides on exocytosis from bovine chromaffin cells (Figure 5B and C). Application of ATP (100 μM) resulted in a marked decrease in vesicle fusion (Figure 5B). This inhibitory effect of ATP on exocytosis was completely blocked by the $P2Y_{12}$ specific antagonist ARC69931MX (Figure 5C).

Cloning of the bovine P2Y12 receptor. Taken together the pharmacological data obtained from bovine chromaffin cells suggest that the purine receptor responsible for inhibition of I_{Ca} and exocytosis is most similar to that of $P2Y_{12}$ or $P2Y_{13}$ except that ATP was a full agonist rather than a weak partial agonist (Marteau *et al.*, 2003) and PPADS is an antagonist. Unlike the pharmacology of the nucleotide responses observed in the P2Y receptors expressed in bovine chromaffin cells, human $P2Y_{13}$ is unresponsive to both 2-MeSATP and ATP (Communi *et al.*, 2001). Human $P2Y_{12}$ however is responsive to 2-MeSATP in the nM range and ATP in the μM range (Takasaki *et al.*, 2001). We therefore cloned the bovine $P2Y_{12}$

receptor in order to compare its pharmacology with the purine sensitive $G_{i/o}$ coupled P2Y

receptor expressed in bovine chromaffin cells. A PCR product of 1145bp was amplified from

bovine chromaffin cell cDNA using the primers 2ndby12fullfor and 2ndby12fullrev. This

sequence is available in the EMBL database under the accession number AJ623293. The

sequence contained an open reading frame of 339 amino acids with a consensus Kozak

sequence at the starting methionine. CLUSTAL alignment of the deduced bovine $P2Y_{12}$

amino acid sequence with human, rat and mouse P2Y receptors confirmed that this sequence

corresponds to $P2Y_{12}$ and not to a related receptor such as $P2Y_{13}$ or $P2Y_{14}$ (Figure 6A). The

cloned bovine receptor showed strong sequence identity to the known mammalian $P2Y_{12}$

sequences with percent identities of 89.4, 84.4 and 85.9 % for human, rat and mouse $P2Y_{12}$

sequences respectively. Alignment of the human and bovine $P2Y_{12}$ amino acid sequences

(Figure 6B) demonstrates the positions of the 37 residues that differ between species. There

are no differences in amino acid sequence in the region from TM6 through to TM7, a region

that has been previously implicated in agonist binding in the $P2Y_2$ receptor (Erb *et al.*, 1995)

Measurements of potassium currents in Xenopus oocytes expressing the bovine $P2Y_{12}$

receptor. Co-expression in *Xenopus* oocytes of the cloned cardiac inward rectifier subunits

Kir 3.1 and Kir 3.4 resulted in robust expression of an inwardly rectifying potassium channel

(Fig 7A). Activation of this channel by $G_{\beta\gamma}$ release was utilised to characterise the

pharmacology of the cloned bovine $P2Y_{12}$ receptor. In order to confirm the absence of

endogenous oocyte channels or receptors that could interfere with results by coupling to the

exogenous bovine $P2Y_{12}$ receptor or rat Kir channels, non-injected oocytes, and oocytes

injected with cRNA for the bovine $P2Y_{12}$ receptor only or only the Kir 3.1 and Kir 3.4 cRNAs

were tested. These oocytes showed no nucleotide evoked currents (data not shown). When

oocytes were co-injected with cRNAs for the bovine $P2Y_{12}$ receptor (50 pg) and rat Kir 3.1

+3.4 channels (1.25 ng each) nucleotide evoked currents were observed. These currents reached a peak within 30 seconds, did not desensitise with the continued agonist application and decayed back to baseline within 3 minutes of agonist removal.

Concentration response data where obtained by utilising the voltage protocol depicted in Figure 7A (and described in detail in materials and methods). Similar to the agonist profile obtained in bovine chromaffin cells, ATP and ADP were essentially equipotent at the cloned bovine $P2Y_{12}$ receptor showing EC_{50} values of 3.74 μM (pEC_{50} 5.47 ± 0.10) and 1.56 μM (pEC_{50} 5.97 ± 0.17) respectively (Figure 7B). 2-MeSADP and 2-MeSATP were considerably more potent with EC_{50} values of 0.28 nM (pEC_{50} 9.55 ± 0.10) and 0.84 nM (pEC_{50} 9.31 ± 0.21) respectively. Uridine nucleotides showed varying degrees of potency with UDP a full agonist (EC_{50} 105.5 μM, pEC_{50} 4.12 ± 0.64), UTP a very weak partial agonist (~10% maximal UDP response with 10mM UTP) and UMP inactive.

The effects of the antagonists ARC69931MX and PPADS were also determined at the cloned $P2Y_{12}$ receptor in *Xenopus* oocytes (Figure 7C). The $P2Y_{12}$ specific antagonist ARC69931MX completely blocked responses of the bovine $P2Y_{12}$ receptor to 10μM ADP (IC_{50} 0.78 nM, pIC_{50} 8.67 ± 0.06) and 10 μM ATP (IC_{50} 2.1 nM pIC_{50} 9.14 ± 0.44). Furthermore, the responses to 1 mM UDP, a concentration normally eliciting a 100% response, was blocked completely by 1 μM ARC69931MX (n=4 oocytes, data not shown). PPADS, a non-specific P2 receptor antagonist blocked responses to 1nM 2MeSATP with an IC_{50} of 1.71 μM (pIC_{50} 5.80 ± 0.05).

Detection of P2Y receptor mRNA in bovine chromaffin cells by RT-PCR. Of the nine known mammalian P2Y receptors ($P2Y_{1, 2, 4, 6, 11, 12, 13, 14 \text{ and } 15}$) it was possible to design sequence specific primers for Bovine $P2Y_{1, 2, 6, 12 \text{ and } 14}$ (Table 1). Amplicons of the expected size were obtained for all primer pairs when PCR was performed on bovine genomic DNA (data not

shown). Three primer pairs (P2Y$_{1,12 \text{ and } 14}$) gave amplicons of the expected size when RT-PCR was performed on first strand cDNA prepared from isolated bovine chromaffin cells (Figure 8). Faint bands were observed in amplifications using P2Y$_2$ and P2Y$_6$ primers. However these bands were not of the correct size and are therefore likely to correspond to non specific amplifications. No bands were observed in control reactions minus reverse transcriptase confirming the absence of contaminating genomic DNA. Thus, from the RT-PCR analysis, transcripts for P2Y$_{1,12 \text{ and } 14}$ but not P2Y$_2$ or P2Y$_6$ could be detected in bovine chromaffin cells.

DISCUSSION

Like other classical neurotransmitters, it is now clear that post-synaptic receptors for nucleotides exist as either ligand-gated ion channels (ATP sensitive P2X receptors), ideally suited to rapid neurotransmission, or G protein coupled P2Y receptors, suited to slower modulatory roles. Evidence for presynaptic nucleotide receptors in the peripheral and central nervous system is also accumulating (Cunha and Ribeiro, 2000; Boehm and Kubista, 2002; Zhang *et al.*, 2003). Positive identification of the receptor subtypes mediating presynaptic effects of nucleotides has however, been complicated by a lack of selective pharmacological tools and paucity of data from receptor knockout studies. We have shown previously that activation of a PTX-sensitive G$_{i/o}$ protein-coupled P2Y receptor in adrenal chromaffin cells inhibits exocytosis and Ca^{2+} entry through N-type and P/Q-type VOCCs (Powell *et al.*, 2000), a similar mechanism is thought to underlie purinergic presynaptic inhibition of sympathetic neurotransmission. In this study, we have identified one of the inhibitory receptors in chromaffin cells as P2Y$_{12}$. In addition, we have found evidence for a second UTP-preferring receptor which acts in a similar manner. The modulation of VOCCs in chromaffin cells by both nucleotide receptors showed all the characteristic properties of G$_{i/o}$ signalling, namely

sensitivity to voltage and PTX (Dolphin, 2003). This signalling pathway is known to be membrane-delimited, independent of diffusible second messengers and to involve direct coupling between the receptor, $G_{i/o}$ $\beta\gamma$ subunits and intracellular domains found on the α1A and α1B pore forming subunits that make up neuronal N- and P/Q-VOCCs.

Similar inhibition of N-type VOCCs by heterologously expressed $P2Y_{12}$ and the closely related $P2Y_{13}$ receptor has also been reported (Simon *et al*., 2002; Kubista *et al*., 2003; Wirkner *et al*. 2004). In the chromaffin-like pheochromocytoma (PC12) cell line, inhibition of N-type channels by a $P2Y_{12}$-like receptor is found at the cell soma (Vartian and Boehm, 2001; Kubista *et al*., 2003) as well as in processes (Kulick and von Kugelgen, 2002) where it contributes to an autocrine-paracrine inhibitory loop regulating exocytotic nucleotide release (Moskvina *et al*., 2003). One notable difference between the PC12 receptor and bovine $P2Y_{12}$ receptor is sensitivity to PPADS, we found it to be a competitive antagonist of the bovine receptor where as in PC12 cells, which are rat derived, it is reported to be ineffective (Vartian and Boehm, 2000; Kulick and von Kügelgen, 2002; Unterberger *et al*., 2002). Species differences in the pharmacology of other P2Y receptor subtypes have been reported previously (Sak and Webb, 2002).

In this study, we describe the cloning and characterisation of a new member of the mammalian P2Y receptor family: bovine $P2Y_{12}$. At the amino acid level, the bovine receptor is similar to human $P2Y_{12}$ with 89% of residues identical between species (compared with 85% between human and rat $P2Y_{12}$). The agonist selectivity of the receptor however showed some slight differences to that reported for the human $P2Y_{12}$ receptor, most notably for ATP and UDP. Whether ATP acts as an agonist at human $P2Y_{12}$ is unclear and most likely depends on cell type and receptor density. At purified and reconstituted human $P2Y_{12}$, where nucleotide breakdown has been eliminated, ATP is not an agonist but a low-affinity antagonist (Bodor *et al*., 2003). However, recombinant human $P2Y_{12}$ expressed in Chinese

hamster ovary cells shows an EC_{50} for ATP (~1μM) similar to that reported for native rat

$P2Y_{12}$ in brain endothelial capillary cells (Simon *et al.*, 2002) and to values reported here for

bovine $P2Y_{12}$ in chromaffin cells and oocytes. In those studies where ATP was reported as a

$P2Y_{12}$ agonist, ATP potency is an order of magnitude lower than ADP (Simon *et al.*, 2002).

At bovine $P2Y_{12}$ however, in both native bovine chromaffin cells and *xenopus* oocytes co-

expressing recombinant bovine $P2Y_{12}$ with rat inward rectifying potassium channels, ATP

acts as a full agonist equipotent to ADP. Nucleotide breakdown of ATP to ADP can be

excluded as an explanation of the bovine $P2Y_{12}$ ATP response since for this to be the case, it

would require that 100% of ATP be instantaneously broken down by X*enopus* oocytes and

bovine chromaffin cells in a constant perfusion system and in any case, in the bovine

chromaffin cell system ATP was actually slightly more potent than ADP.

A second difference in agonist selectivity between bovine and human $P2Y_{12}$ was the

sensitivity to UDP. UDP is inactive at human $P2Y_{12}$ (Takasaki *et al.*, 2001; Hollopeter *et al.*,

2001). However, at bovine $P2Y_{12}$ expressed in *Xenopus* oocytes, UDP is full agonist, all be it

with a low potency (EC_{50} ~100μM). Whilst unlikely, a contamination of the commercial UDP

stocks used in this study with 1% ADP or ATP would be enough to explain the UDP

sensitivity observed. In order to rule out this possibility we performed HPLC on UDP alone

and on UDP spiked with ATP and ADP. No contaminating peak in the sample was above

0.01% and no contaminating peak corresponded to either ATP or ADP. We also observed a

small response to UTP in bovine $P2Y_{12}$ expressed in *xenopus* oocytes (~10% maximal

response to 10mM UTP) at such high concentrations of UTP, the possibility that responses

were due to breakdown of UTP to UDP could not be ruled out.

The UTP receptor inhibiting I_{Ca} and exocytosis in chromaffin cells has not been

identified at the molecular level. UTP does not appear to be acting as a partial agonist at the

bovine P2Y$_{12}$ receptor since it was insensitive to ARC69931MX, caused no shift in the 2-MeSATP concentration-response curve and showed no cross-desensitisation with the purine receptor in chromaffin cells, and had a very low potency at the cloned receptor. Heterologously expressed P2Y$_{2,4,6}$ receptors have also been shown to inhibit I$_{Ca}$ in a neuronal expression system (Filippov *et al.*, 2003;Filippov *et al.*, 1999). However there are notable differences between the results from the expression studies and those found with the endogenous receptor in chromaffin cells, thus even when over expressed in neurones P2Y$_{2,4,6}$ maintain their ability to couple to PTX-insensitive G$_q$ proteins and inhibit M potassium currents which would lead to an increase in [Ca^{2+}]$_i$. UTP does not cause calcium mobilization or entry in chromaffin cells, indicating that it is not acting through a G$_q$ or PLC-coupled receptor in these cells. Furthermore, inhibition of I$_{Ca}$ by heterologously expressed P2Y$_4$ is lost in whole cell recording of neurones, where as the receptor in chromaffin cell showed no such sensitivity to intracellular dialysis. In view of the fact that a positive RT-PCR result was obtained for P2Y$_{14}$ expression in bovine chromaffin cells (Figure 8), we considered the possibility that UTP could be acting as a low potency agonist at the bovine P2Y$_{14}$ receptor in chromaffin cells. However, UDP-glucose, the cognate ligand for human P2Y$_{14}$, gave no response when tested in bovine chromaffin cells (unpublished data). Thus, either bovine P2Y$_{14}$ does not couple to VOCCs in bovine chromaffin cells or the P2Y$_{14}$ RT-PCR product originated from non translated mRNA in chromaffin cells or from P2Y$_{14}$ in a contaminating cell type. It is interesting to note that UTP inhibition of VOCCs has been observed in parasympathetic neurones (Abe *et al.*, 2003) and evidence for a presynaptic inhibitory UTP receptor on sympathetic nerves of the rat and mouse vas deferens has also been reported (Von Kügelgen *et al.*, 1989; Forsyth *et al.*, 1991). Further studies will be required to determine whether one of the still-orphaned GPCRs that share significant sequence identity with the

P2Y$_{12}$ receptor represent a pyrimidine selective G$_{i/o}$ coupled P2Y receptor in the ever growing P2 receptor family.

Finally, the results from this study confirm that P2Y$_{12}$ receptors, the targets of antithrombotic agents, are not restricted to platelets but are also expressed in neuro-endocrine cells where they act as inhibitory receptors to regulate the activity of neuronal VOCCs and vesicular neurotransmitter release. Expression of these receptors at nerve terminals could serve as an important autocrine inhibitory feedback loop to regulate neurotransmission in the periphery and mediate heterosynaptic suppression in the central nervous system.

Legends

Fig. 1. P2Y inhibition of I_{Ca} in adrenal chromaffin cells. A, representative current traces from a single cell demonstrating ATP (10 μM) inhibition of I_{Ca} evoked by 20 ms voltage steps from -90 mV to a test potential of +20 mV at a frequency of 0.067 Hz. Currents were recorded at time points illustrated in B. The rapidly inactivating (< 3ms) inward currents seen at the beginning of the traces are due to opening of TTX-sensitive voltage-activated Na^+ channels; these currents have been truncated for illustrative purposes only. B, diary plots of the effect of ATP on normalized Ca^{2+} entry (filled circles) as measured by integrating I_{Ca}, and corresponding holding current (open circles), measured at -90 mV, 3 ms prior to application of the voltage step. Data shown are the mean of four cells ± s.e.m. The time of agonist application is indicated by the bar above the graph. C, superimposed current traces recorded in a single chromaffin cell before (solid grey line) and during (solid black line) application of UTP (100 μM) in response to a 20 ms test pulse from -90 mV to +20 mV. Preceding the test pulse by a 20 ms depolarization to +120 mV (dashed line) reversed the inhibition by UTP. D, superimposed current traces from a PTX-treated chromaffin cell before (solid grey line, labelled C) and during application of UTP (100 μM) (solid black line). E, superimposed current traces from another PTX treated chromaffin cell recorded before (solid grey line, labelled C) and during application of 2-MeSATP (100 nM) (solid black line). PTX treatment completely blocked the inhibitory effects of nucleotides of I_{Ca}.

Fig. 2. Involvement of Ca^{2+} mobilising P2 receptors. A, Representative fluorescence measurements of cytosolic $[Ca^{2+}]_i$, changes measured with Fura 2 (expressed as the ratio of emission at 340/380 nm) from a single un-clamped chromaffin cell following perfusion with ATP (100 μM), UTP (100μM), histamine (100 μM) and Angiotensin II (300 nM) as indicated

24

by bars above the trace. B, Mean change in resting $[Ca^{2+}]_i$, produced by the indicated agonists for n= 10 cells. Neither ATP nor UTP elicits a change in resting $[Ca^{2+}]_i$, in chromaffin cells.

Fig. 3. Concentration-response curves for the inhibition of I_{Ca} by various nucleotides. A, the percentage inhibition in integrated Ca^{2+} entry through I_{Ca} produced by a series of nucleotide agonists is shown. Each agonist concentration was applied for 2-3 minutes until an equilibrium response was observed, and then washed for 5-10 minutes to ensure full reversal of the inhibition. All points represent the mean ± s.e.m of 3-15 chromaffin cells, lines drawn through the data represent the best fit to the Hill equation. B, effect of UTP on the concentration-response curve for 2-MeSATP inhibition of I_{Ca}. Each point represents the mean ± s.e.m of 4 cells. UTP (10 µM) was co-applied for 2 min with increasing concentrations of 2-MeSATP (10 pM – 10 nM). UTP did not change the maximum response produced by 2-MeSATP, showing that the responses were non-additive, nor did it produce a significant shift in the concentration-response curve.

Fig. 4. Inhibition of VOCCs by 2-MeSATP and UTP differ in their desensitisation characteristics. VOCCs were evoked at a frequency of 0.067 Hz by a 20 ms depolarisation from -90 mV to +20 mV. Data shown are the means of three separate experiments. A, 2-MeSATP (100 nM) was applied for 2 min and then washed out. UTP (100 µM) was then continuously applied for 15 min to induce desensitisation of the response. At the end of the 15 minute desensitisation period, 2-MeSATP was re-applied for a further 2 minutes to examine whether cross desensitisation had occurred. A further UTP application followed to determine recovery from desensitisation. B, converse experiment in which the order of agonist applications were switched, as indicated.

Fig. 5. P2Y$_{12}$ inhibition of VOCCs and exocytosis. A. Concentration response curves for the inhibition of I$_{Ca}$ in chromaffin cells exposed to 2-MeSATP in the absence or presence of PPADS. Data in the presence of 10 μM PPADS were constrained to a Hill Slope of 1 and minimum and maximum values of 0 and 48 %, respectively (*dotted line*). Schild regression analysis of the data (not shown) yielded a pA$_2$ value of 6.42 $\pm$ 0.34. Data illustrated is the mean $\pm$ s.e.m of three such experiments. B1, C1 superimposed Ca^{2+} current traces recorded in a single chromaffin cell held at -90 mV and stepped for 200 ms to +20 mV before (solid grey line) and during superfusion with 100 μM ATP (solid black line), in the absence (B1, control) or presence (C1) of 1 μM ARC69931MX. B2, C2, corresponding ΔC$_m$ recorded in response to currents shown in B1 and C1. Gaps in the C$_m$ traces represent when a voltage step was applied; the increases in C$_m$ that follow Ca^{2+} entry provide a measure of exocytosis corresponding to 2fF per vesicle fusion.

Fig. 6. Bovine P2Y$_{12}$ sequence analysis. A. Phylogenetic analysis of bovine P2Y$_{12}$. P2Y amino acid sequences available for human (h), mouse (m), rat (r) and bovine (b) were aligned using the programme CLUSTAL. Accession numbers for the sequences used in the alignment are as follows: mP2Y$_2$ P35383, rP2Y$_2$ P41232, bP2Y$_2$ O18951, hP2Y$_2$ P41231, mP2Y$_4$ Q9JJS7, rP2Y$_4$ O35811, hP2Y$_4$ P51582, mP2Y$_6$ Q9ERK9, rP2Y$_6$ Q63371, hP2Y$_6$ Q15077, hP2Y$_{12}$ Q9H244, bP2Y$_{12}$ AJ623293, mP2Y$_{12}$ Q9CPV9, rP2Y$_{12}$ Q9EPX4, hP2Y$_{13}$ Q9BPV8, mP2Y$_{13}$ NP_083084, mP2Y$_{14}$ Q9ESG6, rP2Y$_{14}$ O35881, hP2Y$_{14}$ Q15391, mP2Y$_1$ P49650, rP2Y$_1$ P49651, hP2Y$_1$ P47900, bP2Y$_1$ P48042, hP2Y$_{11}$ Q96G91. B. Alignment of the human (Hum) and bovine (Bov) P2Y$_{12}$ amino acid sequences. Residues differing between the two sequences are shaded in the human sequence. Transmembrane domains 1-7 are indicated as lines.

Fig. 7. Concentration response data for the bovine $P2Y_{12}$ receptor co-expressed with rat Kir 3.1 and Kir 3.4 channels in *xenopus* oocytes. Two-electrode voltage clamp recordings were made from oocytes expressing bovine $P2Y_{12}$, rat Kir 3.1 and rat Kir 3.4. A, Currents recorded in response to UDP, 2-MeSATP, and ATP. Oocytes were clamped at 0 mV during the initial agonist application and recovery periods between applications. One minute after agonist application commenced, the holding potential was stepped down to -60mV for 5 seconds and the peak current recorded. A ramp from -60mV to +90mV over 2 seconds was applied after the 5 second recording period. No agonist induced currents or rectification was observed in oocytes expressing bovine $P2Y_{12}$ alone. B, Concentration response curves for the bovine $P2Y_{12}$ receptor expressed in xenopus oocytes co-expressing the rat Kir 3.1 and Kir3.4 channels. Mean currents were normalised to 100 μM ADP (maximal response). Error bars show ± standard error. n= 5-6 oocytes. C, the sensitivity of bovine $P2Y_{12}$ to the antagonists PPADS and ARC69931 was determined in *xenopus* oocytes co-expressing the rat Kir3.1 and Kir 3.1 channels. Recordings were made at a holding membrane potential of –60mV using the protocol depicted in A. Currents in response to an EC_{90} application of agonist (10 μM for ADP and ATP; 1nM for 2-MeSATP) were recorded in the presence of varying concentrations of antagonists and are expressed as a percentage of the EC_{90} response obtained in the absence of antagonist. The $P2Y_{12}$ specific antagonist ARC69931MX completely blocked responses of the bovine $P2Y_{12}$ receptor to 10μM ADP and 10 μM ATP with IC_{50} values of 0.78 nM (pIC_{50} 8.67± 0.06) and 2.1 nM (pIC_{50} 9.14 ± 0.44) respectively. PPADS, a non-specific P2 receptor antagonist blocked responses to 1nM 2-MeSATP with an IC_{50} of 1.71μM (pIC_{50} 5.80 ± 0.05). n=4-5 oocytes.

Fig. 8. RT-PCR analysis of total RNA isolated bovine chromaffin cells. Primers used corresponded to the bovine $P2Y_{1, 2, 6, 12 \text{ and } 14}$ and are detailed in table 1. Control reactions

without reverse transcriptase (-) were run alongside cDNA templates (+) to verify that

amplification was not from genomic DNA. Positive bands of the expected size were observed

for $P2Y_{1,12 \text{ and } 14}$ (marked with asterisks). M: molecular mass marker (size in base pairs).

References

Abbracchio MP, Boeynaems J M, Barnard E A, Boyer J L, Kennedy C, Miras-Portugal M T, King B F, Gachet C, Jacobson K A, Weisman G A and Burnstock G (2003) Characterization of the UDP-glucose receptor (re-named here the $P2Y_{14}$ receptor) adds diversity to the P2Y receptor family. *Trends Pharmacol Sci* **24**:52-5.

Abe M, Endoh T and Suzuki T (2003) Extracellular ATP-induced calcium channel inhibition mediated by P1/P2Y purinoceptors in hamster submandibular ganglion neurons. *Br J Pharmacol* **138**:1535-1543.

Bodor ET, Waldo G L, Hooks S B, Corbitt J, Boyer J L and Harden T K (2003) Purification and functional reconstitution of the human $P2Y_{12}$ receptor. *Mol Pharmacol* **64**:1210-1216.

Boehm S and Kubista H (2002) Fine tuning of sympathetic transmitter release via ionotropic and metabotropic presynaptic receptors. *Pharmacol Rev* **54**: 43-99.

Boyer JL, Zohn I E, Jacobson K A and Harden T K (1994) Differential effects of P2-purinoceptor antagonists on phospholipase C- and adenylyl cyclase-coupled P2Y-Purinoceptors. *Br J Pharmacol* **113**:614-620.

Brinson AE and Harden T K (2001) Differential regulation of the uridine nucleotide-activated $P2Y_4$ and $P2Y_6$ receptors. *J Biol Chem* **276**:11939-11948.

Carabelli V, Carra I and Carbone E (1998) Localized secretion of ATP and opioids revealed through single Ca^{2+} channel modulation in bovine chromaffin cells. *Neuron* **20**:1255-1268.

Charlton SJ, Brown C A, Weisman G A, Turner J T, Erb L and Boarder M R (1996) Cloned and transfected $P2Y_4$ receptors: characterization of a suramin and PPADS-insensitive response to UTP. *Br J Pharmacol* **119**: 1301-1303.

Cheek TR, Morgan A, O'Sullivan A J, Moreton R B, Berridge M J and Burgoyne R D (1993) Spatial localization of agonist-induced Ca^{2+} entry in bovine adrenal chromaffin cells: different patterns induced by histamine and angiotensin II, and relationship to catecholamine release. *J Cell Science* **105**: 913-921.

Communi D, Gonzalez N S, Detheux M, Brezillon S, Lannoy V, Parmentier M and Boeynaems J M (2001) Identification of a novel human ADP receptor coupled to G_i. *J Biol Chem* **276**: 41479.

Cunha RA and Ribeiro J A (2000) ATP as a presynaptic modulator. *Life Sci* **68**:119-137.

Currie KP and Fox A P (1996) ATP serves as a negative feedback inhibitor of voltage-gated Ca^{2+} channel currents in cultured bovine adrenal chromaffin cells. *Neuron* **16**:1027-1036.

Diverse-Pierluissi M, Dunlap, K and Westhead EW(1991). Multiple actions of extracellular ATP on calcium currents in cultured bovine chromaffin cells. *Proc.Natl.Acad.Sci.*USA **88**:1261-1265.

Dolphin AC (2003) G protein modulation of voltage-gated calcium channels. *Pharmacol Rev* **55**: 607-627.

Erb L, Garrad R, Wang Y, Quinn T, Turner J T and Weisman G A (1995) Site-directed mutagenesis of P2U purinoceptors. Positively charged amino acids in transmembrane helices 6 and 7 affect agonist potency and specificity. *J Biol Chem* **270**: 4185-4188.

Fidler N and Fernandez J M (1989) Phase tracking: an improved phase detection technique for cell membrane capacitance measurements. *Biophys J* **56**: 1153-1162.

Filippov AK, Simon J, Barnard E A and Brown D A (2003) Coupling of the nucleotide P2Y$_4$ receptor to neuronal ion channels. *Br J Pharmacol* **138**: 400-406.

Filippov AK, Webb T E, Barnard E A and Brown D A (1999) Dual coupling of heterologously-expressed rat P2Y$_6$ nucleotide receptors to N-type Ca^{2+} and M-type K$^+$ currents in rat sympathetic neurones. *Br J Pharmacol* **126**: 1009-17.

Forsyth KM, Bjur R A and Westfall D P (1991) Nucleotide modulation of norepinephrine release from sympathetic nerves in the rat *vas deferens*. *J Pharm Exp Ther* **256**: 821-826.

Gandia L, Garcia AG, and Morad M (1993) ATP modulation of calcium channels in chromaffin cells. *J.Physiol*. **470**:55-72.

Harvey RJ and Darlison M G (1991) Random-Primed CDNA synthesis facilitates the isolation of multiple 5'-CDNA ends by RACE. *Nucleic Acids Res* **19**: 4002.

Henderson DJ, Elliot D G, Smith G M, Webb T E and Dainty I A (1995) Cloning and characterisation of a bovine P2Y receptor. *Biochem Biophys Res Commun* **212**: 648-56.

Hollopeter G, Jantzen H M, Vincent D, Li G, England L, Ramakrishnan V, Yang R B, Nurden P, Nurden A, Julius D and Conley P B (2001) Identification of the platelet ADP receptor targeted by antithrombotic drugs. *Nature* **409**: 202-7.

Inbe H, Watanabe S, Miyawaki M, Tanabe E, and Encinas JA. Identification and Characterization of a Cell-Surface Receptor, P2Y$_{15}$, for AMP and Adenosine. *J.Biol.Chem* **279:** 19790-19799

Ingall AH, Dixon J, Bailey A, Coombs M E, Cox D, McInally J I, Hunt S F, Kindon N D, Teobald B J, Willis P A, Humphries R G, Leff P, Clegg J A, Smith J A and Tomlinson W (1999) Antagonists of the platelet P2T receptor: a novel approach to antithrombotic therapy. *J Med Chem* **42**: 213-220.

Kubista, H., Lechner, S., and Boehm, S. Attenuation of the P2Y receptor-mediated control of neuronal Ca2+ channels by antithrombotic drugs. (2003). *Br J Pharmacol*. **138**: 343-50

Kulick MB and von Kügelgen, I (2002) P2Y-Receptors Mediating an inhibition of the evoked entry of calcium through N-type calcium channels at neuronal processes. *J Pharmacol Exp Ther* **303**: 520-526.

Marteau F, Le Poul E, Communi D, Communi D, Labouret C, Savi P, Boeynaems J M and Gonzalez N S (2003) Pharmacological characterization of the human P2Y$_{13}$ Receptor. *Mol Pharm* **64**: 104.

Moskvina E, Unterberger U and Boehm S (2003) Activity-dependent autocrine-paracrine activation of neuronal P2Y receptors. *J Neurosci* **23**: 7479-7488.

North RA (2002) Molecular physiology of P2X receptors. *Physiol Rev* **82**: 1013-67.

Powell AD, Teschemacher A G and Seward E P (2000) P2Y Purinoceptors inhibit exocytosis in adrenal chromaffin cells via modulation of voltage-operated calcium channels. *J Neurosci* **20**: 606-616.

Sak K and Webb T E (2002) A retrospective of recombinant P2Y receptor subtypes and their pharmacology. *Arch Biochem Biophys* **397**: 131-6.

Simon J, Filippov A K, Goransson S, Wong Y H, Frelin C, Michel A D, Brown D A and Barnard E A (2002) Characterization and channel coupling of the P2Y$_{12}$ nucleotide receptor of brain capillary endothelial cells. *J Biol Chem* **277**: 31390-31400.

Takasaki J, Kamohara M, Saito T, Matsumoto M, Matsumoto S, Ohishi T, Soga T, Matsushime H and Furuichi K (2001) Molecular cloning of the platelet P2T(AC) ADP receptor: pharmacological comparison with another ADP Receptor, the P2Y$_1$ receptor. *Mol Pharmacol* **60**: 432-439.

Teschemacher AG and Seward E P (2000) Bidirectional modulation of exocytosis by angiontensin II involves multiple G-protein-regulated transduction pathways in adrenal chromaffin cells. *J Neurosci* **20**: 4776-4785.

Unterberger U, Moskvina E, Scholze T, Freissmuth M and Boehm S (2002) Inhibition of adenylyl cyclase by neuronal P2Y receptors. *Br J Pharmacol* **135**: 673-684.

Vartian N and Boehm S (2001) P2Y receptor-mediated inhibition of voltage-activated Ca^{2+} currents in PC12 cells. *Eur J Neurosci* **13**: 899-908.

Von Kügelgen I, Schoffel E and Starke K (1989) Inhibition by nucleotides acting at presynaptic P2-receptors of symapthetic neuro-effector transmission in the mouse isolated vas deferens. *Naunyn-Schmiedeberg's Arch Pharmacol* **340**: 522-532.

Wirkner K, Schweigel J, Gerevich Z, Franke H, Allgaier C, Barsoumian E L, Draheim H and Illes P (2004) Adenine nucleotides inhibit recombinant N-type calcium channels via G protein-coupled mechanisms in HEK 293 cells; involvement of the P2Y$_{13}$ receptor-type. *Br J Pharmacol* **141**: 141-151.

Zhang Jm, Wang H k, Ye C q, Ge W, Chen Y, Jiang Z l, Wu C p, Poo MM and Duan S (2003) ATP released by astrocytes mediates glutamatergic activity-dependent heterosynaptic suppression. *Neuron* **40**: 971-982.

Legends

Fig. 1. P2Y inhibition of I_{Ca} in adrenal chromaffin cells. A, representative current traces from a single cell demonstrating ATP (10 µM) inhibition of I_{Ca} evoked by 20 ms voltage steps from -90 mV to a test potential of +20 mV at a frequency of 0.067 Hz. Currents were recorded at time points illustrated in B. The rapidly inactivating (< 3ms) inward currents seen at the beginning of the traces are due to opening of TTX-sensitive voltage-activated Na^+ channels; these currents have been truncated for illustrative purposes only. B, diary plots of the effect of ATP on normalized Ca^{2+} entry (filled circles) as measured by integrating I_{Ca}, and corresponding holding current (open circles), measured at -90 mV, 3 ms prior to application of the voltage step. Data shown are the mean of four cells ± s.e.m. The time of agonist application is indicated by the bar above the graph. C, superimposed current traces recorded in a single chromaffin cell before (solid grey line) and during (solid black line) application of UTP (100 µM) in response to a 20 ms test pulse from -90 mV to +20 mV. Preceding the test pulse by a 20 ms depolarization to +120 mV (dashed line) reversed the inhibition by UTP. D, superimposed current traces from a PTX-treated chromaffin cell before (solid grey line, labelled C) and during application of UTP (100 µM) (solid black line). E, superimposed current traces from another PTX treated chromaffin cell recorded before (solid grey line, labelled C) and during application of 2-MeSATP (100 nM) (solid black line). PTX treatment completely blocked the inhibitory effects of nucleotides of I_{Ca}.

Fig. 2. Involvement of Ca^{2+} mobilising P2 receptors. A, Representative fluorescence measurements of cytosolic $[Ca^{2+}]_i$, changes measured with Fura 2 (expressed as the ratio of emission at 340/380 nm) from a single un-clamped chromaffin cell following perfusion with ATP (100 µM), UTP (100µM), histamine (100 µM) and Angiotensin II (300 nM) as indicated

24

by bars above the trace. B, Mean change in resting $[Ca^{2+}]_i$, produced by the indicated agonists

for n= 10 cells. Neither ATP nor UTP elicits a change in resting $[Ca^{2+}]_i$, in chromaffin cells.

Fig. 3. Concentration-response curves for the inhibition of I_{Ca} by various nucleotides. A, the

percentage inhibition in integrated Ca^{2+} entry through I_{Ca} produced by a series of nucleotide

agonists is shown. Each agonist concentration was applied for 2-3 minutes until an

equilibrium response was observed, and then washed for 5-10 minutes to ensure full reversal

of the inhibition. All points represent the mean ± s.e.m of 3-15 chromaffin cells, lines drawn

through the data represent the best fit to the Hill equation. B, effect of UTP on the

concentration-response curve for 2-MeSATP inhibition of I_{Ca}. Each point represents the

mean ± s.e.m of 4 cells. UTP (10 µM) was co-applied for 2 min with increasing

concentrations of 2-MeSATP (10 pM – 10 nM). UTP did not change the maximum response

produced by 2-MeSATP, showing that the responses were non-additive, nor did it produce a

significant shift in the concentration-response curve.

Fig. 4. Inhibition of VOCCs by 2-MeSATP and UTP differ in their desensitisation

characteristics. VOCCs were evoked at a frequency of 0.067 Hz by a 20 ms depolarisation

from -90 mV to +20 mV. Data shown are the means of three separate experiments. A, 2-

MeSATP (100 nM) was applied for 2 min and then washed out. UTP (100 µM) was then

continuously applied for 15 min to induce desensitisation of the response. At the end of the

15 minute desensitisation period, 2-MeSATP was re-applied for a further 2 minutes to

examine whether cross desensitisation had occurred. A further UTP application followed to

determine recovery from desensitisation. B, converse experiment in which the order of

agonist applications were switched, as indicated.

Fig. 5. P2Y$_{12}$ inhibition of VOCCs and exocytosis. A. Concentration response curves for the inhibition of I$_{Ca}$ in chromaffin cells exposed to 2-MeSATP in the absence or presence of PPADS. Data in the presence of 10 µM PPADS were constrained to a Hill Slope of 1 and minimum and maximum values of 0 and 48 %, respectively (*dotted line*). Schild regression analysis of the data (not shown) yielded a pA$_2$ value of 6.42 ± 0.34. Data illustrated is the mean ± s.e.m of three such experiments. B1, C1 superimposed Ca^{2+} current traces recorded in a single chromaffin cell held at -90 mV and stepped for 200 ms to +20 mV before (solid grey line) and during superfusion with 100 µM ATP (solid black line), in the absence (B1, control) or presence (C1) of 1 µM ARC69931MX. B2, C2, corresponding ΔC$_m$ recorded in response to currents shown in B1 and C1. Gaps in the C$_m$ traces represent when a voltage step was applied; the increases in C$_m$ that follow Ca^{2+} entry provide a measure of exocytosis corresponding to 2fF per vesicle fusion.

Fig. 6. Bovine P2Y$_{12}$ sequence analysis. A. Phylogenetic analysis of bovine P2Y$_{12}$. P2Y amino acid sequences available for human (h), mouse (m), rat (r) and bovine (b) were aligned using the programme CLUSTAL. Accession numbers for the sequences used in the alignment are as follows: mP2Y$_2$ P35383, rP2Y$_2$ P41232, bP2Y$_2$ O18951, hP2Y$_2$ P41231, mP2Y$_4$ Q9JJS7, rP2Y$_4$ O35811, hP2Y$_4$ P51582, mP2Y$_6$ Q9ERK9, rP2Y$_6$ Q63371, hP2Y$_6$ Q15077, hP2Y$_{12}$ Q9H244, bP2Y$_{12}$ AJ623293, mP2Y$_{12}$ Q9CPV9, rP2Y$_{12}$ Q9EPX4, hP2Y$_{13}$ Q9BPV8, mP2Y$_{13}$ NP_083084, mP2Y$_{14}$ Q9ESG6, rP2Y$_{14}$ O35881, hP2Y$_{14}$ Q15391, mP2Y$_1$ P49650, rP2Y$_1$ P49651, hP2Y$_1$ P47900, bP2Y$_1$ P48042, hP2Y$_{11}$ Q96G91. B. Alignment of the human (Hum) and bovine (Bov) P2Y$_{12}$ amino acid sequences. Residues differing between the two sequences are shaded in the human sequence. Transmembrane domains 1-7 are indicated as lines.

Fig. 7. Concentration response data for the bovine $P2Y_{12}$ receptor co-expressed with rat Kir 3.1 and Kir 3.4 channels in *xenopus* oocytes. Two-electrode voltage clamp recordings were made from oocytes expressing bovine $P2Y_{12}$, rat Kir 3.1 and rat Kir 3.4. A, Currents recorded in response to UDP, 2-MeSATP, and ATP. Oocytes were clamped at 0 mV during the initial agonist application and recovery periods between applications. One minute after agonist application commenced, the holding potential was stepped down to -60mV for 5 seconds and the peak current recorded. A ramp from -60mV to +90mV over 2 seconds was applied after the 5 second recording period. No agonist induced currents or rectification was observed in oocytes expressing bovine $P2Y_{12}$ alone. B, Concentration response curves for the bovine $P2Y_{12}$ receptor expressed in xenopus oocytes co-expressing the rat Kir 3.1 and Kir3.4 channels. Mean currents were normalised to 100 μM ADP (maximal response). Error bars show ± standard error. n= 5-6 oocytes. C, the sensitivity of bovine $P2Y_{12}$ to the antagonists PPADS and ARC69931 was determined in *xenopus* oocytes co-expressing the rat Kir3.1 and Kir 3.1 channels. Recordings were made at a holding membrane potential of –60mV using the protocol depicted in A. Currents in response to an EC_{90} application of agonist (10 μM for ADP and ATP; 1nM for 2-MeSATP) were recorded in the presence of varying concentrations of antagonists and are expressed as a percentage of the EC_{90} response obtained in the absence of antagonist. The $P2Y_{12}$ specific antagonist ARC69931MX completely blocked responses of the bovine $P2Y_{12}$ receptor to 10μM ADP and 10 μM ATP with IC_{50} values of 0.78 nM (pIC_{50} 8.67± 0.06) and 2.1 nM (pIC_{50} 9.14 ± 0.44) respectively. PPADS, a non-specific P2 receptor antagonist blocked responses to 1nM 2-MeSATP with an IC_{50} of 1.71μM (pIC_{50} 5.80 ± 0.05). n=4-5 oocytes.

Fig. 8. RT-PCR analysis of total RNA isolated bovine chromaffin cells. Primers used corresponded to the bovine $P2Y_{1, 2, 6, 12 \text{ and } 14}$ and are detailed in table 1. Control reactions

27

without reverse transcriptase (-) were run alongside cDNA templates (+) to verify that

amplification was not from genomic DNA. Positive bands of the expected size were observed

for P2Y$_{1,12 \text{ and } 14}$ (marked with asterisks). M: molecular mass marker (size in base pairs).
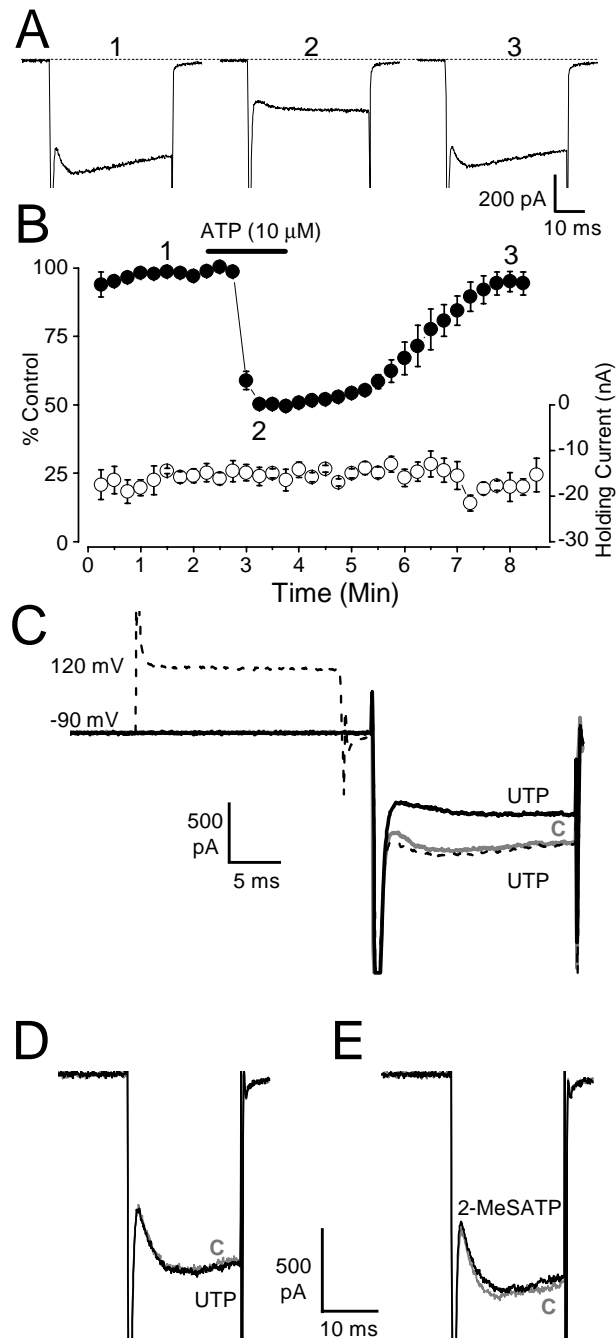
Table 1

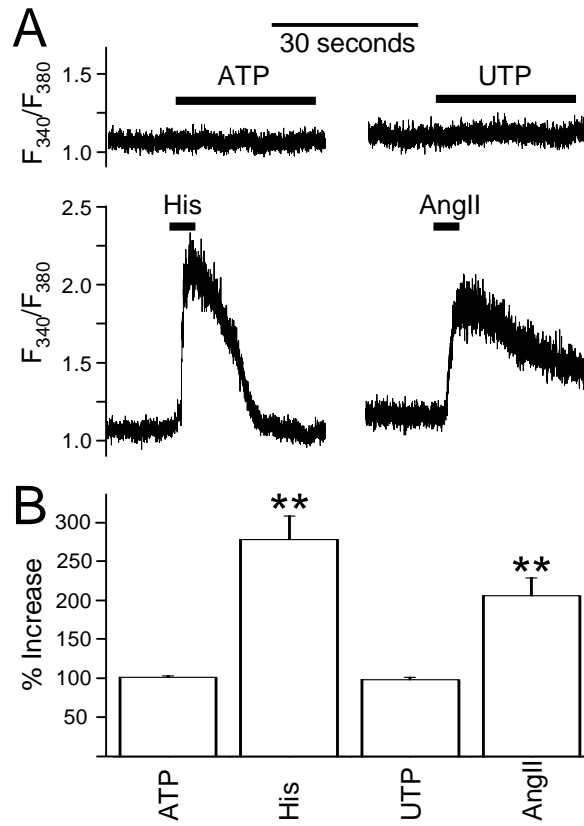**Table 1.** Primer sequences used for RT-PCR analysis of P2Y expression in bovine chromaffin cells

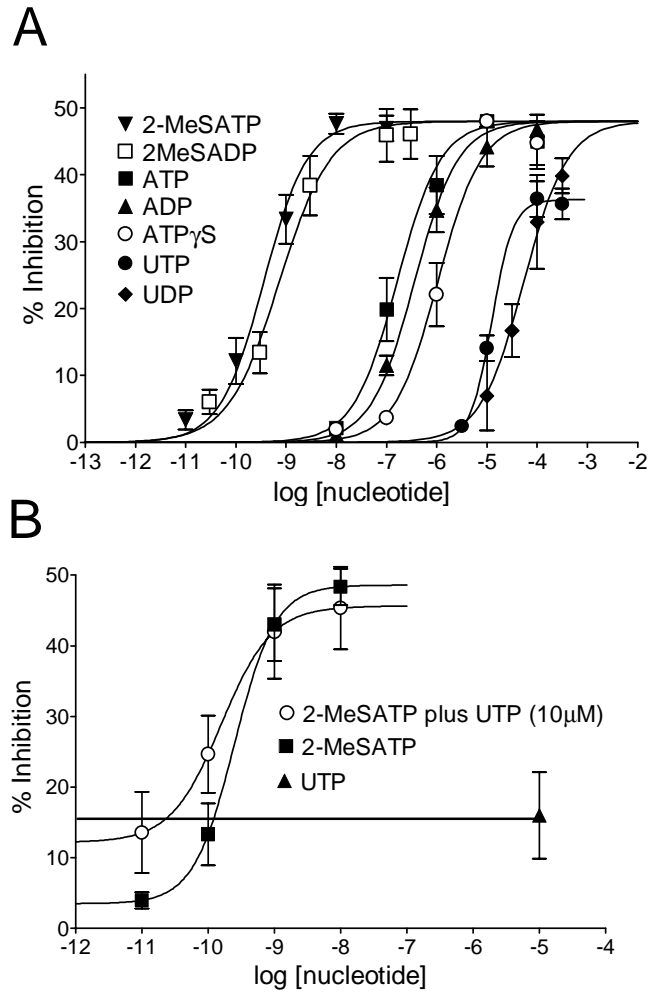| Gene	Forward Primer	Reverse Primer	Expected size (bp)
$P2Y_1$	GCCAGCCCGTTCAAATG	CAGCCCAAAATCAGCACC	599
$P2Y_2$	ACTTCGTCACCACCAGC	GAAAGGCAGAAAGCAGAG	275
$P2Y_6$	CTACTAAGGCGTGCGTTTC	GGGAGCAGGCATACAGC	433
$P2Y_{12}$	TGATCGCTACCAGAAGACCACCAG	TTCATGCCAAACCAGACCAAACTC	205
$P2Y_{14}$	GCATCGTGTTCTTCGGGCTCA	TGTAGGGGATTCTGGCAATGTGGTA	447

Table 2

Table 2. Pharmacological data for endogenous receptors in bovine chromaffin cells and the cloned bovine $P2Y_{12}$ receptor expressed in *Xenopus* oocytes. EC_{50}: Concentration of nucleotide required to elicit half the maximal response. pEC_{50}: -$\log_{10} EC_{50}$ (Molar). Hill Slope: gradient of concentration response. Values show $\pm$ standard error of the mean.

	EC_{50}	pEC50	Hill Slope
Chromaffin cells			
2-MeSADP	0.73 nM	9.14 ± 0.10	0.85 ± 0.14
2-MeSATP	0.49 nM	9.45 ± 0.22	1.13 ± 0.16
ATP	0.35 µM	6.67 ± 0.25	1.24 ± 0.30
ADP	0.39 µM	6.44 ± 0.12	0.93 ± 0.08
UDP	34.86 µM	4.48 ± 0.09	1.53 ± 0.35
UTP	14.24 µM	4.89 ± 0.11	1.92 ± 0.44
ATP γS	1.17 µM	5.99 ± 0.16	1.38 ± 0.13
Oocytes			
2-MeSADP	0.28 nM	9.55 ± 0.10	0.63 ± 0.06
2-MeSATP	0.84 nM	9.31 ± 0.21	0.66 ± 0.06
ATP	3.74 µM	5.47 ± 0.10	0.87 ± 0.04
ADP	1.56 µM	5.97 ± 0.17	0.86 ± 0.11
UDP	105.5 µM	4.12 ± 0.64	0.91 ± 0.54
UTP**	50.12 µM	4.30 ± 0.40	

** Weak Partial Agonist

MOL#224 **Figure 1**

Figure 2

MOL#224 **Figure 3**

Figure 4

MOL#224 **Figure 5**

MOL#224 **Figure 6**

A

```
                              mP2Y2
                              rP2Y2
                              bP2Y2
                              hP2Y2
                              mP2Y4
                              rP2Y4
                              hP2Y4
                              mP2Y6
                              rP2Y6
                              hP2Y6
                              hP2Y12
                              bP2Y12
                              mP2Y12
                              rP2Y12
                              hP2Y13
                              mP2Y13
                              mP2Y14
                              rP2Y14
                              hP2Y14
                              mP2Y1
                              rP2Y1
                              hP2Y1
                              bP2Y1
                              hP2Y11
```
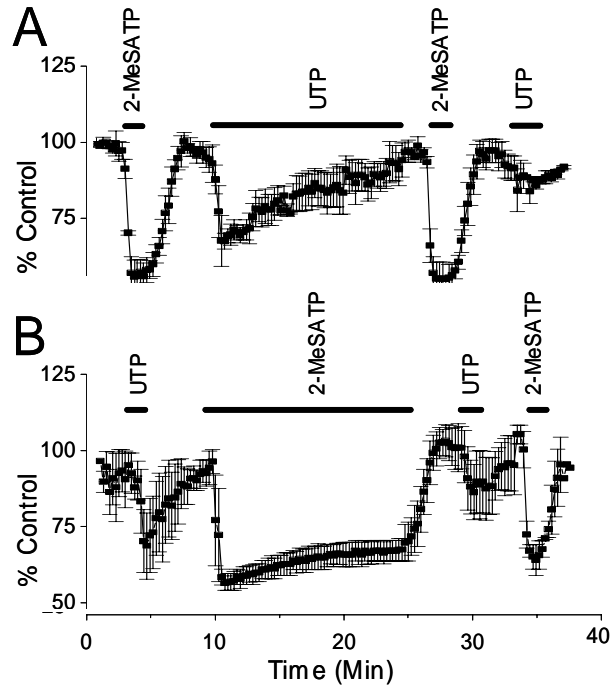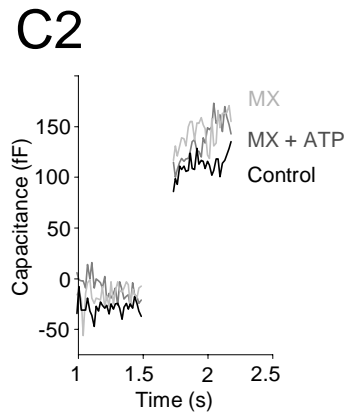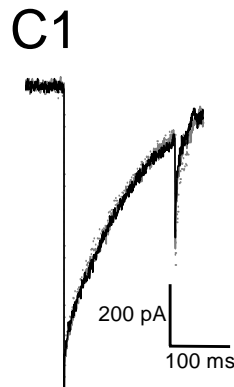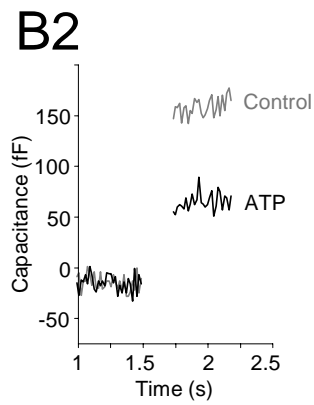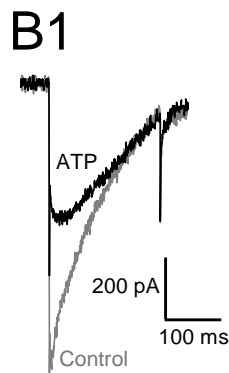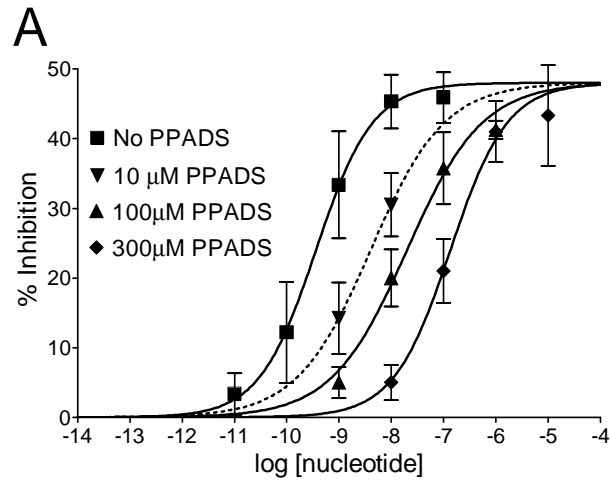
B

```
  1  M---DNLTSVAGNNSQCSRDYKITQVLFPLLYTVLFFVGL  Bov
  1  MQAVDNLTSAPGNTSLCTRDYKITQVLFPLLYTVLFFVGL  Hum
                                         TM1

 38  ITNSLAMRIFSQIRSKSNFIIFLKNTVISDLLMILTFPFK  Bov
 41  ITNGLAMRIFFQIRSKSNFIIFLKNTVISDLLMILTFPFK  Hum
                                         TM2

 78  ILSDTKLGTGPLRAFVCQVTSVVFHFTMYISISFLGLITI  Bov
 81  ILSDAKLGTGPLRTFVCQVTSVIYFTMYISISFLGLITI   Hum
                                         TM3

118  DRYQKTTRPFKTANPNNLLGAKILSVVIWAFMFLISLPNM  Bov
121  DRYQKTTRPFKTSNPKNLLGAKILSVVIWAFMFLLSLPNM  Hum
                                         TM4

158  ILTNRRPSDKTVKKCSFLKSEFGLVWHEIVNYVCQVIFWI  Bov
161  ILTNRQPRDKNVKKCSFLKSEFGLVWHEIVNYICQVIFWI  Hum
                                         TM5

198  NFLIVIVCYTLITKELYKSYVRTRGAGKVPKKKVNIKVFI  Bov
201  NFLIVIVCYTLITKELYRSYVRTRGVGKVPRKKVNVKVFI  Hum

238  IIAVFFICFVPFHFARIPYTLSQTRDVFDCTAENTLFYVK  Bov
241  IIAVFFICFVPFHFARIPYTLSQTRDVFDCTAENTLFYVK  Hum
        TM6

278  ESTLWLTSLNACLDPFIYFFLCKSFKNSLMSMLRCSNSTS  Bov
281  ESTLWLTSLNACLDPFIYFFLCKSFRNSLISMLKCPNSAT  Hum
        TM7

318  PPSHDNRKKGQDGSDPSEETPM  Bov
321  SLSQDNRKKEQDGGDPNEETPM  Hum
```
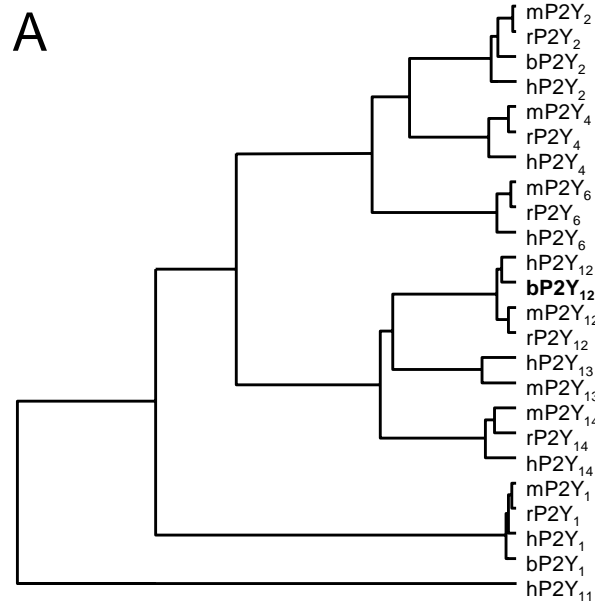
Figure 7

MOL#224

Figure 8